Optics & Laser Technology 193 (2026) 114154

Contents lists available at ScienceDirect

Optics and Laser Technology

journal homepage: www.elsevier.com/locate/optlastec

Full length article

Measurement of linewidth and noise dependence on the optical feedback parameter C by means of an FM-Converted Self-Mix interferometer

Parisa Esmaili [a], Michele Norgia [a,*], Alfred Albert [d], San-Liang Lee [b,d], Silvano Donati [b,c]

[a] Dipartimento di Elettronica, Informazione e Bioingegneria, Politecnico di Milano, I-20133 Milan, Italy
[b] HiSiPIC of NTUST (National Taiwan University of Science and Technology), Taipei, Taiwan
[c] Dipartimento di Ingegneria Industriale e Informatica, Università di Pavia 27100 Pavia, Italy
[d] NTUST (National Taiwan University of Science and Technology), Taipei, Taiwan

ARTICLE INFO

Keywords:
Semiconductor lasers
Optical feedback
Interferometry
Optical measurements

ABSTRACT

Using a frequency-converted self-mix interferometer, we analyze with a new comprehensive approach, and then confirm with measurement results, the dependence of Schawlow-Townes (S-T) linewidth, frequency uncertainty linewidth and frequency noise spectral density from the optical feedback (or Acket's) parameter C. Theoretically, the S-T linewidth and the noise spectral density are both dependent on $(1 + C)^{-2}$, whereas the frequency uncertainty varies as $(1 + C)^{-1}$. We test these dependences with new original measurements, taken on two laser diodes with different emission wavelengths and linewidth and find excellent agreement with the theory.

1. Introduction

Self-Mixing Interferometry (SMI) is an interferometric technique that measures the effects of a small back-injection in a laser cavity [1]. It can be employed to measure optical phase shifts in a number of applications, ranging from mechanical metrology to vibration sensing, to biological motility measurements and to consumer applications, and several good tutorial and reviews have been published in last year's [2–4]. Recently, it has been shown [5–7] that using the frequency modulation (FM) signal instead of the amplitude modulation (AM) signal greatly improves the Signal-to-Noise Ratio (SNR) of the phase measurement, and that at increasing level of optical feedback the spectral density of frequency noise decreases appreciably [8]. Thanks to the measurement of the FM signal induced in the laser, it is possible to improve the resolution of a self-mixing interferometer by about two orders of magnitude, allowing to reach performances typical of high-level instruments, unthinkable with the simple measurement of AM-SMI. The drawback of this implementation is the added complexity of the optical setup, requiring an FM-to-AM converter. Our approach is to implement a Mach-Zehnder interferometer as frequency discriminator [8]. In order to realize a compact system, recently the FM-to-AM conversion has been proposed also with integrated silicon nitride edge filters [9], or in an all-fiber system employing Bragg grating [7].

In this paper we develop the topic further, with an original derivation of the relationship between spectral density of frequency fluctuations and linewidth and find their dependence on the *C*-factor describing the optical feedback [2]. Then, for the first time at the best of our knowledge, we validate the theoretical results through SMI experiments carried out with two different laser diodes, and show that the optical feedback actually improves the SNR of frequency-converted SMI measurements, and the frequency-fluctuations linewidth by a factor $(1 + C)$, and moreover the frequency power spectral density and the intrinsic Schawlow-Townes linewidth of the laser by a factor $(1 + C)^2$. The benefits brought to SMI measurements are: an SNR improved by $(1 + C)$ and a distance of operation (as limited by coherence length) improved by $(1 + C)^2$. The results obtained in this work allow to design an FM-SMI by anticipating the achievable performances as a function of the laser used.

The paper is structured as follows: in the next Section we offer a new derivation of the linewidths and the frequency spectral density, in Sect. III we discuss the impact of feedback, in Sect. IV we describe the setup of the frequency-conversion SMI, and in Sect. V we report the result of original measurements of frequency noise power spectral density and S-T linewidth at several *C*-factors, showing for the first time an excellent agreement with the theoretical prediction; finally, we draw some conclusions.

* Corresponding author.
E-mail address: michele.norgia@polimi.it (M. Norgia).

https://doi.org/10.1016/j.optlastec.2025.114154
Received 7 July 2025; Received in revised form 13 October 2025; Accepted 16 October 2025
Available online 24 October 2025

2. Linewidth of frequency fluctuations and schawlow-townes linewidth

Preliminarily, let's consider the shape of the laser line, for a laser oscillating on the cavity with a decay time τ_{cav}. When lifetime broadening is the only mechanism determining the linewidth, it is well-known that the line shape is Lorentzian [10], the decay of the field is exponential, $\exp(-\tau/\tau_{cav})$, and the frequency line shape is $L(\nu) = 1/[1+(2\pi\nu\tau_{cav})^2]$, with HWHM (half-width half-maximum) given by

$$HWHM = 1/(2\pi\tau_{cav}) \quad (1)$$

In the case of Doppler broadening, the decay is Gaussian, with a distribution $\exp[-\tau^2/(2\tau_{cav}^2)]$, and the frequency line shape which is again a Gaussian, $L(\nu) = \exp\text{-}2\tau_{cav}^2(\pi\nu)^2$, and the half-width half-maximum (HWHM) is $\Delta\nu_{cav}=(2\ln 2)^{1/2}/(2\pi\tau_{cav})$.

Frequently, the line shape is the convolution of Lorentzian and Gaussian distributions, and $\Delta\nu_{cav} = b/(2\pi\tau_{cav})$, with the factor b intermediate between 1 and $\sqrt{(2\ln 2)} = 1.177$.

Now, let's calculate the linewidth due to frequency fluctuations. This is the practical case of a laser clock, when we count periods of the laser oscillation, and of the frequency-converted SMI signal where we use a step frequency filtering to recover the FM component of the SMI [6]. Let's consider N photons in the cavity, produced by a power P and observed in a time T. Then, the observed average frequency will have an uncertainty $\Delta\nu_n = \Delta\nu_{cav}/\sqrt{N}$. Letting $N = P/(h\nu)T$, and using Shannon's relation with bandwidth B $T = 1/(2B)$, we get the frequency uncertainty for the linewidth:

$$\Delta\nu_n = \Delta\nu_{cav}\sqrt{2Bh\nu/P} \quad (2)$$

and this $\Delta\nu_n$ will be a HWHM if $\Delta\nu_{cav}$ is a HWHM too.

Next, to find the linewidth $\Delta\nu_{S\text{-}T}$ of the laser emission – usually called the Schawlow –Townes linewidth – we use Wiener-Khintchine (W-K) theorem and calculate the square of pulsation linewidth $\Delta\Omega_{S\text{-}T} = 2\pi\Delta\nu_{S\text{-}T}$ as the product of spectral density of pulsation $S(\Omega)$ times the bandwidth of fluctuations allowed by the system, which is again $\Delta\Omega_{S\text{-}T}$. Equating the terms, we have $S(\Omega)\Delta\Omega_{S\text{-}T} = \Delta\Omega_{S\text{-}T}^2$, or [11]:

$$S(\Omega) = \Delta\Omega_{S-T} \quad (3)$$

On its turn, the spectral density of frequency $S(\nu)$is given by the variance divided by bandwidth, or $\Delta\nu_n^2/2B$, so that $S(\Omega=(2\pi)^2S(\nu)= (2\pi)^2\Delta\nu_n^2/2B$. Using (2) and (3) we obtain $\Delta\Omega_{S\text{-}T} = 2\pi\Delta\nu_{S\text{-}T} =(2\pi)^2\Delta_{cav}^2 (h\nu/P)$, or the Schawlow –Townes' famous expression [10,12]:

$$\Delta\nu_{S-T} = 2\pi h\nu\Delta\nu_{cav}^2/P \quad (4)$$

(Note: (4) already includes the ½ correction factor later found by Lax). The value of $\nu_{S\text{-}T}$ a HWHM if $\Delta\nu_{cav}^2$ is a HWHM too.

The half-width has to be used instead of the (usual) standard deviation because linewidth may follow a Lorentz distribution, with infinite standard deviation because of the long tails. When the distribution has finite quadratic value, like for a Gaussian or a Voigt (convolution of Gaussian and Lorentz) distribution, the HWHM is close to the standard deviation value $\Delta\nu_{rms}$. In addition, if we simply cut out the long tail at say, 1 % of the maximum, also the variance of the Lorentzian line becomes finite, and the distribution is not much different from the Gaussian.

Several interesting points shall be noted. First, despite the similarity, $\Delta\nu_{S\text{-}T}$ and $\Delta\nu_n$ have totally different meaning: the former gives the natural spread of frequency of the laser emission, i.e., is the distribution of frequency emitted instant after instant by the laser. It is observed, for example, on an optical spectrum analyzer; thus, it determines the coherence properties. The coherence length is indeed [10,12]:

$$L_c = c/\pi\Delta\nu_{S-T} \quad (5)$$

(with a $\Delta\nu_{S\text{-}T}$ a FWHM value); whereas the latter is the uncertainty of frequency observed (and averaged) on a time $1/2B$ or bandwidth B. As said, this is the case describing the uncertainty of the measurand 'frequency' like for example in self-mixing FM-to-AM converted signal [7], or the error signal in external cavity interrogation signal for wavelength stabilization and is subjected to reduction by averaging [13], thus it coincides with the two-sample Allan's rms value of frequency deviations observed on time intervals $1/2B$, denoted as $\sigma_v(2, 1/2B,\nu)$ [7].

Second, by reversing the passages, from (4) we obtain (2), i.e. a new derivation of the Schawlow-Townes (S-T) linewidth based only on statistical reasoning and W-K theorem.

Third, we can also obtain (4) from the Heisenberg principle [10,12], as in the original derivation of Schawlow –Townes, by writing it in the form $\delta\Omega \geq 1/(N_d\tau_{cav})$ (see [12], eq.8), where $\delta\Omega = 2\pi\Delta\nu_{S\text{-}T}$ and $N_d = P/(h\nu)\tau_{cav}$ so that $2\pi\Delta\nu_{S\text{-}T} \geq 1/[P/(h\nu)\tau_{cav}]\tau_{cav}$; with $\tau_{cav} = 1/(2\pi\Delta\nu_{cav})$ we re-obtain (4).

Last, note the different trend of the two uncertainties with the number of photons: $\Delta\nu_{cav}$ has the inverse and $\Delta\nu_n$ the inverse square root proportionality with N. In general, the relation between the two linewidths is

$$\Delta\nu_n = \sqrt{\Delta\nu_{S-T}B/\pi} \quad (6)$$

Another useful relation connects the S-T linewidth $\Delta\nu_{S\text{-}T}$ to the power spectral density of frequency $S(\nu)$ given, in view of the Wiener-Khintchine theorem, by the square frequency fluctuation $\Delta\nu_n^2$ divided by the bandwidth B, or $S(\nu) = \Delta\nu_n^2/B$. Indeed, from the experimental measurement of $S(\nu)$, we can trace back the S-T linewidth (4) as [12]:

$$\Delta\nu_{S-T} = \pi S(\nu) \quad (7)$$

and this is another method to determine $\Delta\nu_{S\text{-}T}$, and from here, the coherence length.

$L_c = c/(\pi\Delta\nu_{S\text{-}T})$

Further refinements to the above results come from taking account of non-idealities [10] like: (i) the incomplete inversion factor $g=N_2/(N_2 – N_1)$, and (ii) the enhancement $(1 + \alpha^2)$ of the linewidth due to the Kramer-Kronig relation between absorption and dispersion, which transfers itself to frequency the amplitude fluctuations, and where α is known as the linewidth enhancement factor or Henry's factor. Taking account of these effects, (2) and (5) are rewritten as:

$$\Delta\nu_n = \sqrt{g(1+\alpha^2)}\Delta\nu_{cav}\sqrt{2Bh\nu/P} \quad (8)$$

$$\Delta\nu_{S-T} = g\left(1+\alpha^2\right)2\pi h\nu\Delta\nu_{cav}^2/P \quad (9)$$

The above results are obtained under the tacit assumption that power spectral density $S(\Omega)$, or $S(\nu)$ as in (7), is constant in frequency ν, that is the frequency noise is white.

Experimentally it is always found an $1/f$ component for $S(\nu)$, which is dominant up to a corner frequency ν_c. Laurent et al. [11] has found that the white part of the spectrum contributes to give a linewidth (7) and a Lorentz distribution for the line, whereas the $1/f$ component contributes to a Gaussian distributed line and has a width $\Delta\nu_{1/f} = \sqrt{4\pi\nu_c S(\nu_c)}$. The resulting distribution is the convolution of the two lines, known as a Voigt distribution [14].

Finally, it is worth noting that the above results are generally valid for a laser, regardless of the operation of FM- SMI.

3. Impact of optical feedback on linewidths

The above linewidths are valid for a solitary, unperturbed laser. When the laser emitting a field E_0 is subjected to feedback by a fraction $\eta = E_s/E_0$ of field returning into the cavity from a remote target, the linewidths are affected, and the governing parameter is Acket's feedback factor C defined as [4]:

$$C = \left(1+\alpha^2\right)\eta K(\tau_{ext}/\tau_{in}) \quad (10)$$

where $K = \eta_s(1 - r_2^2)(r_3/r_2)$ is the fraction of field coupled into the oscillating mode, in terms of mirrors (field) reflectivity (r_2 and r_3) and

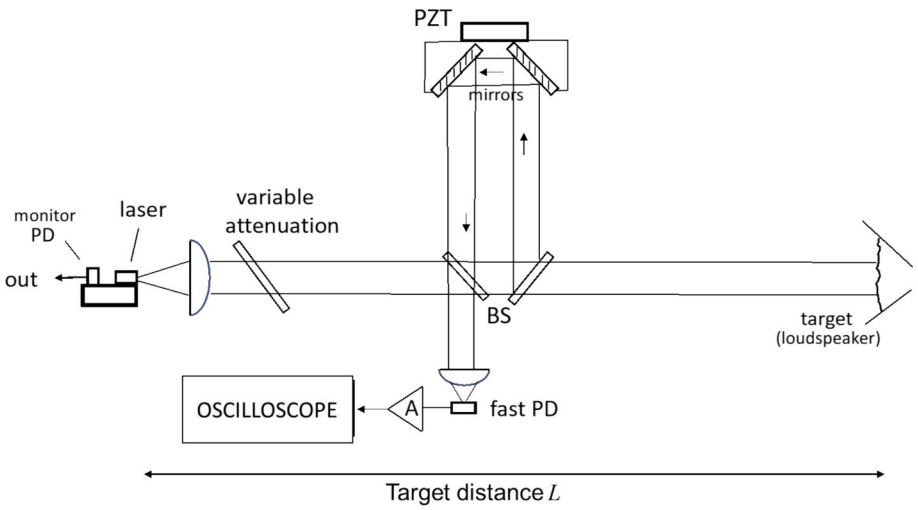

Fig. 1. The setup for the measurement of the fm-converted signal.

mode superposition factor η_s, and τ_{ext}/τ_{in} is the ratio of external roundtrip propagation time $\tau_{ext} = 2L/c$ to the target at a distance L, divided by the roundtrip time internal to the laser cavity $\tau_{in} = 2n_{las}L_{las}/c$ [4].

Schunk and Petermann [15], Petermann et al. [16], Tkach and Chraplyvy [17] and J. Kitching et al. [18] have extensively studied the problem of linewidth affected by feedback, starting from the Lang and Kobayashi equations [19]. As the exact solution looked impracticable, useful results have been obtained by numerical simulations [15,16] of the equations, finding that at moderate feedback ($C < 1$) the Schawlow −Townes linewidth is either narrowed or widened according to the value of phase shift to the target $\phi = 2kL$ ($k = 2\pi/\lambda$ being the wavevector), and that the feedback-perturbed $\Delta\nu_{S\text{-}T(F)}$ is accurately described by the following law, extrapolated from the results of extensive simulations:

$$\Delta\nu_{S-T}(F) = \Delta\nu_{S-T} \Big/ [1 + C\cos(\phi + atan\alpha)]^2 \tag{11}$$

This is the regime of Region I of the Tkach and Chraplyvy (T-C) diagram [17] of optical feedback.

As new contribution of this paper (to the best of our knowledge), we derive (11) from the second L-K (Lang and Kobayashi) equation [19], written as

$$\phi_0 = \phi + C\sin(\phi + atan\alpha) \tag{12}$$

where ϕ_0 and ϕ are respectively the unperturbed and perturbed phases of the laser oscillation, given by $\phi_0 = 2\pi\nu_0\tau_{ext}$ and $\phi = 2\pi\nu\tau_{ext}$. Substituting in (12) it is:

$$2\pi\nu_0\tau_{ext} = 2\pi\nu\tau_{ext} + C\sin(2\pi\nu\tau_{ext} + atan\alpha) \tag{13}$$

Frequency fluctuations are introduced in the L-K equations by a Langevin noise term [19], that makes the instantaneous frequency become $\nu + \Delta\nu$. The fluctuation $\Delta\nu$ is found by taking the differential at both sides of (14) and dropping the $2\pi\tau_{ext}$ terms. In this way, we get:

$$\Delta\nu_0 = \Delta\nu + C[\cos(2\pi\nu\tau_{ext} + atan\alpha]\Delta\nu \tag{14}$$

Or

$$\Delta\nu = \Delta\nu_0/[1 + C\cos(2\pi\nu\tau_{ext} + atan\alpha)] \tag{15}$$

Uncertainty $\Delta\nu$ is the frequency deviation under feedback, whereas $\Delta\nu_0$ is the unperturbed frequency deviation. Taking the squares at both members of (15) and recalling (6), we can write the relation for the (feedback) perturbed and unperturbed S-T linewidths as:

$$\Delta\nu_{ST(F)} = \Delta\nu_{ST} \Big/ [1 + C\cos(2\pi\nu\tau_{ext} + atan\alpha)]^2 \tag{16}$$

which coincides with Eq.8.

Additionally, in view of (7), the frequency spectral density under optical feedback also condition becomes scaled by the factor in square brackets:

$$S_{(F)}(\nu) = S(\nu) \Big/ [1 + C\cos(2\pi\nu\tau_{ext} + atan\alpha)]^2 \tag{17}$$

At increased feedback, that is for $C > 1$, we enter in the region II of the T-C diagram where amplitude and frequency exhibit switching because the laser hops on the next external-cavity mode. (15) does not hold anymore because the laser will preferably lock frequency to minimize linewidth, or at $2\pi\nu\tau_{ext} + atan\alpha = 0$, as found by numerical simulations [11,15,17] and confirmed by the experimental observations described below. Therefore, we get:

$$\Delta\nu_{n(F)} = \Delta\nu_0/(1 + C) \tag{18}$$

$$\Delta\nu_{ST(F)} = \Delta\nu_{ST}/\,(1 + C)^2 \tag{18'}$$

$$S_{(F)}(\nu) = S(\nu)/(1 + C)^2 \tag{18''}$$

and obviously, for a measurement made by means of the frequency-converted SMI signal, as the signal is independent from C while noise follows (18), the SNR is increased by factor $1 + C$, that is $SNR_{(F)} = SNR\,(1 + C)$; also important, in view of (5), (7) and (18''), the coherence length is increased of a factor $(1 + C)^2$, that is $L_{c(F)} = L_c\,(1 + C)^2$.

Eqs. (18) still hold in region III of the T-C diagram where oscillation returns to be single mode [17, 20]. Finally, at very high values of C, the laser breaks into chaotic oscillations, in the region IV of the T-C diagram [21], where the linewidth becomes much broadened and the spectral density much increased, so the system is good for another application – chaos cryptography [22] – but of course not good anymore for measurements.

4. Experimental setup

In Fig. 1 we report the setup for the measurement of the frequency-converted SMI signal, the same used in previous papers [5,6]. The optical source is a single mode laser, feeding a beam-splitter to divide the beam in two parts: one (95 % in power) sent to the under measurement (the plain white paper cone of a loudspeaker driven at audio frequency), and the other (5 % in power) to the FM-to-AM converter made by the Mach-Zehnder interferometer (MZI), acting as a steep optical filter. The output of the filter is detected by a fast photodiode with 35 MHz bandwidth, amplified and observed on an electrical spectrum analyzer. Another photodiode, the monitor mounted on the back mirror of the

Table 1
Model and specifications of tested DFB laser diodes.

Laser diode Model	λ [nm]	P_o [mW]	I_{th} [mA]	I_{bias} [mA]	I_w [mA]	P_w [mW]
WSLD1550-020 *m*	1550	20	10	90	30	8
ML720J11S	1310	5	6	20	15	3

laser, is used to observe the SMI waveform when the target is driven by a sine excitation, and to infer the *C* factor. A piezoceramic actuator (PZT) is used to tune the MZI to the laser wavelength.

Two different DFB lasers have been tested, emitting at different wavelengths. Model and specifications of tested laser diodes are reported in Table 1.: nominal power P_o, threshold current I_{th}, nominal current I_{bias}, and the working values I_w and power P_w.

The lasers were fitted in identical collimating tubes, containing an aspheric lens of 4.5-mm diameter and numerical aperture NA = 0.4, producing a near-field beam waist with $w_{\perp}$=1.5 $w_{//}$=0.75 mm (in the D4$\sum$ standard). The drive currents were kept lower than the specification of the manufacturer, to dispense with the use of a temperature controller and also to have a larger modulation index of the self-mixing signal [23].

The MZI has a transmission response given by:

$$T(f) = 1/2[1 + \cos(2\pi f \Delta L/c)] \tag{19}$$

and with a path imbalance of $\Delta L = 45$ cm the free spectral range is FSR $= c/\Delta L = 6.67$ GHz and the maximum slope as at half-fringe and has a value:

$$S_{F(MZI)} = \frac{dT}{df_{(max)}} = \frac{\pi \Delta L}{c} = 4.710^{-9} Hz^{-1} \tag{20}$$

To ensure working on the maximum slope of the MZI cosine transmission, a half-fringe locking circuit has been designed. The circuit dynamically adjusts the pathlength imbalance of the MZI by means of a piezoceramic actuator moving the retroreflecting prism in Fig. 1, as servo loop that maximizes the response (at half fringe) achieved by the photodiode (fast PD in Fig. 1). The output signal is observed at the electrical spectrum analyzer at different values of the feedback parameter *C*.

5. Measurements

For logistic issues, we have carried out the measurement of power spectral density and associated *C* factor at the Politecnico unit, and of linewidth $\Delta\nu$ and *C* at the NTUST unit. In the two units, we have used the same method for the *C*-measurement and samples of the same batch for the diode lasers, fed at the same current. To have the same parameters in

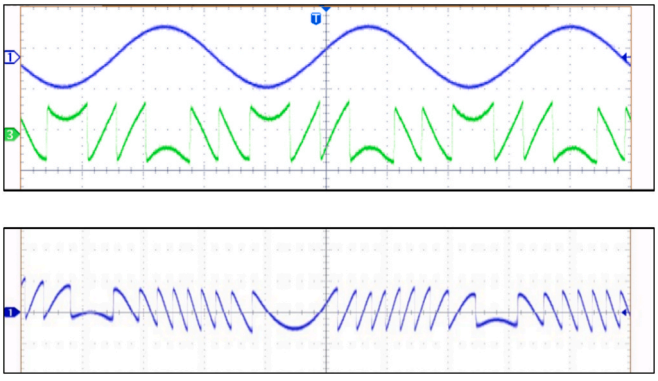

Fig. 2. SMI waveforms of the two lasers for a sine-wave drive of the target displacement (horizontal axis 1 μs/DIV, vertical axis 500 mV/DIV): top the WSLD1550-020 m at $C = 1.3$, bottom the ML720J11S at $C = 1.6$.

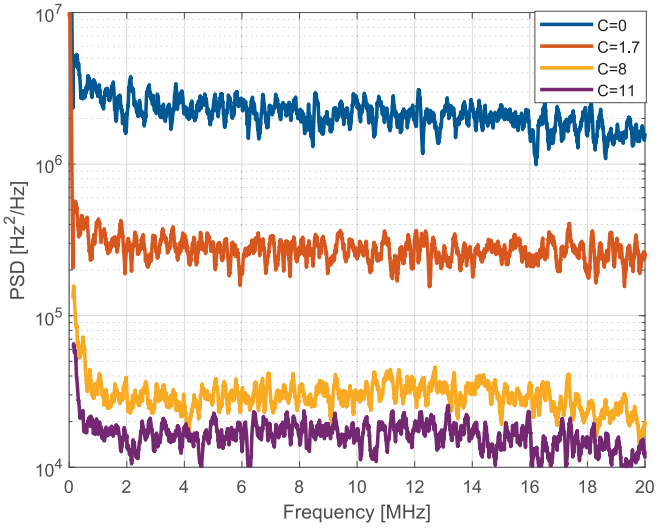

Fig. 3. The measured power spectral density PSD (in Hz^2/Hz) of frequency noise of the DFB laser WSLD1550-020 m for some values of the feedback parameter *C*.

the two measurements, we have used self-mixing-related measurements for *C* and $\Delta\nu$, adapting methods already reported in literature (see below) to be carried out in the frequency-converted setup of Fig. 1. To make the different cases of feedback strength, we have used several distances of the target (typ. 30, 60, 90, 120 cm) as well as placed a focusing lens (20 mm diameter, focal length 20 mm) just in front of the target or using a retroreflecting surface at the target to increase the returning power and thus the *C*-factor of the experiment.

A. Measuring the C factor.

To measure *C*, we used the (slower) monitor photodiode available at the rear mirror of the laser and applied a triangular-wave, low frequency (typ. 10 Hz) excitation to the target, a loudspeaker placed at a distance *L* = 30…120 cm from the laser, of amplitude suitable to generate many periods. A variable attenuator (Fig. 1) allowed to adjust the feedback level and thus the *C* factor.

The *C* factor value was evaluated with the time-intervals method described in [24] for $1 < C < 4$, by measuring the peak-to-zero crossing phase intervals X_{13} and X_{24} on increasing and decreasing semi-periods and inverting the constitutive equations (Eqs. (3a) and (3b) of [24])

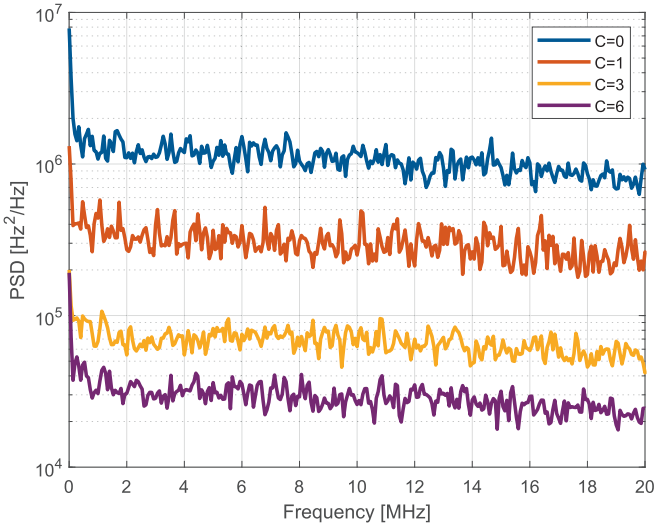

Fig. 4. The measured power spectral density PSD (in Hz^2/Hz) of frequency noise of the DFB laser ML720J11S for some values of the feedback parameter *C*.

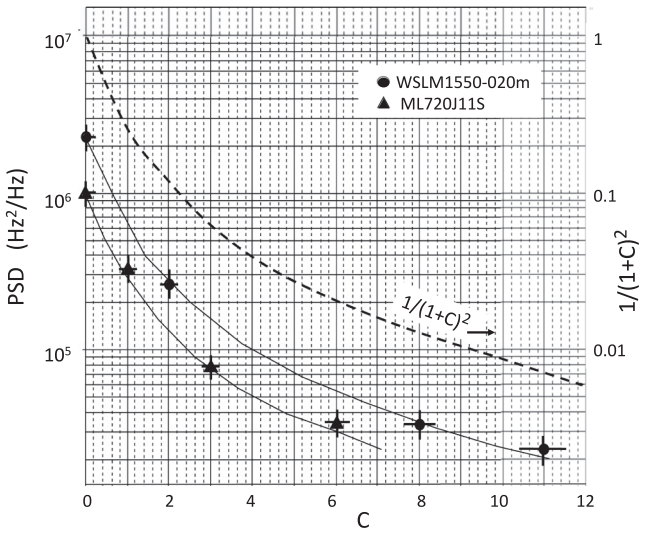

Fig. 5. The PSD of the two lasers considered in this paper, plotted against C and compared to the $1/(1+C)^2$ narrowing factor (dotted line) of PSD. The different scales of the plots, left for PSDs and right for $1/(1+C)^2$ are to better show the matching of the trend.

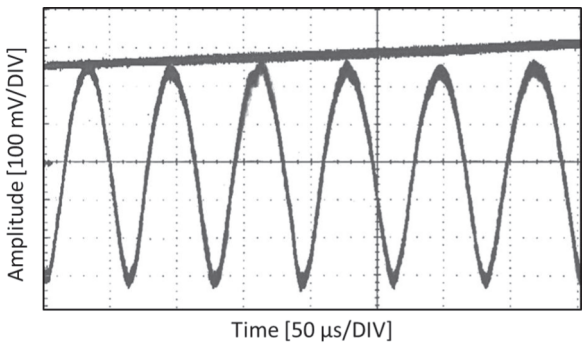

	Value	Mean	Min	Max	St Dev
Period	62.88 µs	62.9678 µs	61.66 µs	64.36 µs	440.8 ns
Frequency	15.9 kHz	15.9919 kHz	15.54 kHz	16.22 kHz	111.2 Hz

Fig. 6. Top panel: oscilloscope acquisition of the SMI (AM component) waveform; bottom panel: the mean value $< T_p >$ and standard deviation σ_p of the SMI signal period, as directly measured by DPO7254 digital oscilloscope (number of samples: 100).

derived from the Lamb and Kobayashi equations, through a simple graphical solution. Specifically, we enter X_{13} and X_{24} in Fig. 5 of [24] and can read from the graph C and α of the experiment. For $C < 1$ we used Eq. (5.43) of [1] (originally introduced by [25]) and for $C > 4$ we inserted a calibrated neutral filter to bring back the laser in the range $1 < C < 4$. The typical estimated accuracy of the measured C value is ± 10 %. For example, in the measurement of linewidth described below (see next Fig. 6.), at sight we can see that $C < 1$ because the self-mixing waveform has no switching, and on the waveform we measure $T_z = 28.2$ µs, and $T_M = 30.4$ µs on a period of $T = 62.9$ µs, whence from Eq. (3.43′) of [1] we find $C = \pi[(T_z\text{-}T)^2+(T_M\text{-}T)^2]^{1/2} = 0.52$, the value of first point for WSLD1550 in Fig. 7. Using the description in [24] it is also possible to determine α, but we focused on the value of C which directly influences the linewidth and hence the noise in the FM-SMI.

Exemplary SMI waveforms of the two lasers (Table 1) are reported in Fig. 2.Fig. 3.

B. Power Spectral Density.

With an Electrical Spectrum Analyzer (included in the oscilloscope DSOX3024T), we measured the power spectral density (PSD) of the frequency-converted SMI signal (the amplifier output in Fig. 1). As shown in Figs. 3 and 4, the PSD of the two DFB lasers had an almost flat component at all C-values in the interval 1–20 MHz and a well-defined $1/f$ component below ≈100 kHz, while the PSD had a modest roll-down in frequency after a much larger $1/f$ component.

To trace back the PSD of frequency (PSD_f) from the PSD measured at the photodiode output (PSD_V), we have divided the power spectral density readings (in V^2/Hz) of the electrical spectrum analyzer by the square of the slope S_{MZI} times the square of the peak-to-peak signal voltage V_{pp}. We get, in formula, $PSD_f = PSD_V / [V_{pp}S_{MZI}]^2$, where $V_{pp} = 2.1$ V is the peak-to-peak amplitude of the SMI signal at the amplifier output, and $V_{pp}S_{MZI} = 9.8{\cdot}10^{-9}$ (V/Hz).

From Figs. 3 and 4, the white noise PSD of the two DFB lasers, WSLD1550 at 1550 nm and ML720J11S at 1300 nm, nearly constant in the frequency range 1 to 20 MHz, have unperturbed ($C = 0$) mean values of 2.2 10^6 Hz^2/Hz and 1.0 10^6 Hz^2/Hz respectively (both with a ± 15 % deviation in the interval) read at the central frequency of 10 MHz.

In the approximation of constant PSD=$S(\nu)$, the corresponding Lorentz linewidths $\Delta\nu_{S\text{-}T} = \pi S(\nu)$ are, in view of (7), 6.9 MHz and 3.1 MHz respectively.

To summarize the results of the measurements, we plot in Fig. 5 the PSD of frequency fluctuations as a function of frequency for the above lasers considered. As we can see, the trend of PSD with the factor $1/(1+C)^2$ is well matched by both sources in the considered intervals of C values.

About the $1/f$ components, the linewidth contribution is, according to Laurent et al. [11], $\Delta\nu_{1/f} = \sqrt{4\pi\nu_c S(\nu_c)}$ where ν_c is the corner frequency of the $1/f$ component. For our two lasers we find 1.4 MHz and 0.8 MHz, values that are 3–4 times less than the Lorentz linewidth due to white noise, and thus introduce only a moderate linewidth increase (<10 %). Indeed, from the quadratic composition of convoluted linewidth, the final result for linewidths read: about 7.0 MHz and 3.2 MHz respectively for the two lasers, and these are the values reported in Fig. 6..

Figs. 3 and 4 pertain to the case of moderate feedback of the T-K diagram. For the case of weak feedback (C < 1) or the region I of the T-K diagram, we have already published a result of measurement, see Fig.9 of [6], showing a minor dependence of PSD from the total phase ($2\pi\nu\tau_{ext}$ + atanα), and we direct the interested reader to this reference.

C. Measuring the laser linewidth.

Recalling (7), the trend of PSD is duplicated by that of the linewidth $\Delta\nu_{S\text{-}T}$ – in the approximation of constant PSD, i.e., of white noise distribution of frequency fluctuations – under the feedback conditions expressed by the C factor. Although already indirectly contained in the PSD dependence from $1/(1+C)^2$, also the linewidth $\Delta\nu_{ST(F)}$ dependence on C, expressed by (18′), deserves a direct check.

Commonly, there are two main options for the linewidth measurement: (i) a Mach-Zehnder self-heterodyne setup using an acousto-optical modulator to move the optical spectrum away from the baseband, at typ. a 30 to 80 MHz carrier, superposed to which we can then detect the laser frequency spectrum as a two-sided distribution; (ii) a simpler Mach-Zehnder self-homodyne setup [26] with arm unbalance $\Delta L > L_c$, to make the laser line beat with itself and generate a one-sided distribution. Even simpler, and suitable for testing laser at different wavelengths (iii) we can measure the linewidth from the time jitter that the period exhibits in the SMI regime, as introduced in [27]. We employed method (iii) and used a commercial instrument (Fiber Optic Interferometer model HP 11980A) based on method (ii) to validate the results on a few values of C.

As an illustration of the used method (iii), Fig. 6. shows a sample of the self-mixing waveform captured by the oscilloscope yielding the computed values of mean period $< T_p >$ and rms deviation σ_p of the period. Thus, the rms of phase deviation is $\sigma_\phi = 2\pi\sigma_p/<T_p>$. Now, we develop the deviation of self-mixing phase $\phi = 2kL$, considering a target at distance L, i.e. $\Delta\phi = 4\pi\ (\Delta\nu/c)L + 2k\Delta L$. In general, the second

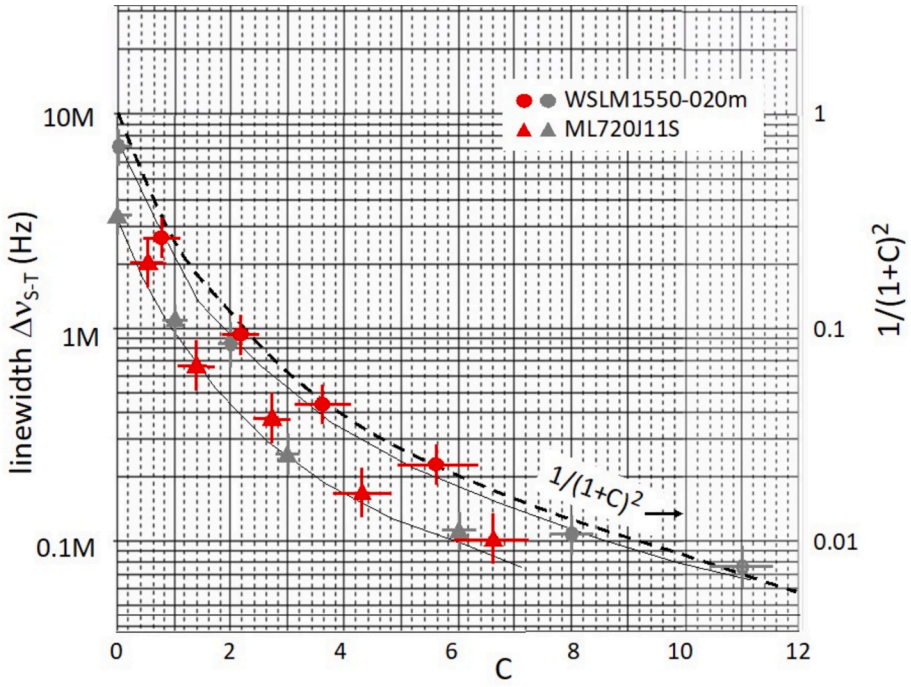

Fig. 7. The measured linewidths of the two lasers (red symbols) plotted against C and compared to the values predicted by (7) (gray symbols) and with the theoretical $(1 + C)^{-2}$ narrowing factor reported for reference (dotted line).

contribution to deviation is not negligible because driven by small vibrations coming from the ambient (or, microphonic effect) and we shall take the derivative respect to L of the $\Delta\phi$ −dependence, as shown in [27] and obtain $d\Delta\phi/dL = 4\pi(\Delta\nu/c)$. As a variant of the method, we used a linear sweep developing a self-mixing signal at a high frequency, f_{sm} = 15 kHz, so that the second term due to microphonic noise at $f_d \approx$5-20 Hz and $\Delta L \approx \lambda$ is small in the measurement time ($\approx \Delta L\, f_d/f_{sm} \approx 10^{-3}\lambda$), and we can disregard it. Thus, we have: $\sigma_\phi = 4\pi\, L\Delta\nu/c$ and can solve for the linewidth as $\Delta\nu = c\sigma_\phi/(4\pi L) = \sigma_\phi 23$ MHz/s (with distance L expressed in m).

As an example, from the digital scope in Fig. 6. we can read $< T_p >$=62.96 μs and σ_p = 0.44 μs, whence σ_ϕ = 0.044 r and $\Delta\nu$ = 0.044 23 M/0.3 = 3.37 MHz, and this is the first point at C = 0.52 of the WSML1550 laser diode curve of Fig. 7.

	Value	Mean	Min	Max	St Dev
Period	62.88 μs	62.9678 μs	61.66 μs	64.36 μs	440.8 ns
Frequency	15.9 kHz	15.9919 kHz	15.54 kHz	16.22 kHz	111.2 Hz

The measured linewidths $\Delta\nu_{S\text{-}T(F)}$ of the two lasers are plotted in Fig. 7 against C along with the values calculated by Eq.4, that is, by shifting of π the ordinate scale of PSD = $\Delta\nu_{S\text{-}T}/\pi$. As it can be seen, the agreement of direct measurement of linewidths and linewidths calculated by Eq.3 from the PSD is surprisingly good.

D. SNR and MDS of the frequency-converted signal.

Finally, we may consider an example of the improvement obtained by the frequency-converted SMI signal, like that reported in [7]. The improvement of noise and of SNR with feedback is here given by a factor $1 + C$, as shown by Eq. (17) of [7], a dependence that was unintentionally checked in Sect. III of [7] with a good match for C = 2.06 when compared to experimental measurements.

In another experiment [28], the SMI vibrometer minimum detectable signal (MDS) at SNR = 1 was MDS_0 = 20 pm in the $C \approx 0$ case, and at the moderate feedback level of C = 1.5 was measured to be 9 pm, in reasonable agreement with the theoretical value $MDS = MDS_0/(1 + C)$ = 20 pm/2.5 = 8 pm.

These results are about two orders of magnitude better than traditional AM-SMI [2–4], even considering the possibility of balanced detection that allows to improve the SNR of amplitude modulation by some dB [29].

6. Conclusions

We have carried out measurements on the effect of optical feedback on the performance of a FM-SMI and found that the governing equations and the dependence on C of linewidth (either Schawlow −Townes' $\Delta\nu_{S\text{-}T}$ or frequency fluctuation $\Delta\nu_n$) and power spectral density of noise, are in excellent agreement with the experimental measurements performed on two different laser diodes. Experimental measurements of the Schawlow-Townes linewidth decrease by $(1 + C)^2$ has been reported previously for both laser diode [30] and quantum cascade lasers [31], but without correlating it to the Allan's frequency uncertainty nor to the frequency noise spectral density like done in this paper.

The results of this paper are the base for FM-SMI measurements with improved SNR and for linewidth-narrowed operation of single-mode lasers.

CRediT authorship contribution statement

Parisa Esmaili: Visualization, Methodology, Investigation, Data curation. **Michele Norgia:** Writing – review & editing, Writing – original draft, Supervision, Methodology, Conceptualization. **Alfred Albert:** Software, Data curation. **San-Liang Lee:** Supervision, Project administration, Funding acquisition. **Silvano Donati:** Writing – review & editing, Writing – original draft, Supervision, Project administration, Methodology, Investigation, Conceptualization.

Declaration of competing interest

The authors declare that they have no known competing financial interests or personal relationships that could have appeared to influence the work reported in this paper.

Acknowledgment

This work has been performed under the NSTC project no. 112-2221-E-011-032-MY3 (R.O.C), and the MICS (Made in Italy–Circular and Sustainable) Extended Partnership and received funding from Next-Generation EU (Italian PNRR– M4 C2, Invest 1.3 – D.D. 1551.11-10-2022, PE00000004). CUP MICS D43C22003120001.

Data availability

No data was used for the research described in the article.

References

[1] S. Donati, Photonic Instrumentation, 2nd ed., CRC Taylor & Francis, Boca Raton, FL, USA, 2023.
[2] T. Taimre, M. Nicolic, K. Bertling, Y.L.T. Bosch, A.D. Rakic, Laser feedback interferometry: a tutorial on the self-mixing effect for coherent sensing, Adv. Opt. Photon. 7 (2015) 570–631, https://doi.org/10.1364/AOP.7.000570.
[3] S. Donati, Developing self-mixing interferometry for instrumentation and measurements, Laser Photon. Rev. 6 (2012) 393–417, https://doi.org/10.1002/lpor.201100056.
[4] Y. Yu, Y. Fan, B. Liu, Self-Mixing Interferometry and Applications, in: Proc. SPIE/COS Photonics Asia, SPIE, 2016. https://doi.org/10.1117/12.2245851.
[5] V. Contreras, J. Lönnquist, J. Toivonen, Edge filter enhanced self-mixing interferometry, Opt. Lett. 40 (2015) 2814–2817, https://doi.org/10.1364/OL.40.002814.
[6] S. Donati, M. Norgia, Self-Mixing Interferometer with a Laser Diode: Unveiling the FM Channel and its Advantages respect to the AM Channel, IEEE J. Quantum Electron. 53 (2017) 1–8, https://doi.org/10.1109/JQE.2017.7500210.
[7] Z. Xie, J. Li, D. Guo, W. Xia, H. Yan, M. Wang, All-fiber laser self-mixing interferometry for signal enhancement with phase-shifted fiber Bragg grating, Optics & Laser Tech. 172 (2024) 110496, https://doi.org/10.1016/j.optlastec.2023.110496.
[8] M. Norgia, V. Contreras, S. Donati, Noise in an FM-Converted Self-Mixing Interferometer, IEEE Trans. Instrum. Meas. 69 (2020) 5100–5106, https://doi.org/10.1109/TIM.2019.2957867.
[9] C. Deleau, et al., Optical Feedback FM-to-AM Conversion with Photonic Integrated Circuits for Displacement Sensing applications, J. Lightwave Technol. 42 (2024) 3446–3453, https://doi.org/10.1109/JLT.2024.3355048.
[10] C.J. McKinstrie, T.J. Stirling, A.S. Helmy, Laser linewidths: tutorial, J. Opt. Soc. Am. B 38 (2011) 3837–3848, https://doi.org/10.1364/JOSAB.38.003837.
[11] P. Laurent, A. Clairon, C. Breant, Frequency noise analysis of optically self-locked diode lasers, IEEE J. Quantum Electron. 25 (1989) 1131–1142, https://doi.org/10.1109/3.24206.
[12] C. Akcay, P. Perrin, J.P. Rolland, Estimation of longitudinal resolution in optical coherence imaging, Appl. Opt. 41 (2002) 5256–5262, https://doi.org/10.1364/AO.41.005256.
[13] E. Di Gaetano, B. Keliehor, K. Gallacher, P.F. Griffin, M. Sorel, 778.1 nm distributed feedback lasers for Rb two-photon atomic systems with sub-4 kHz linewidths, APL Photonics 9 (2024) 056114, https://doi.org/10.1063/5.0191088.
[14] G. Di Domenico, S. Schilt, P. Thomann, Simple approach to the relation between laser frequency noise and laser line shape, Appl. Opt. 49 (2010) 4801–4807, https://doi.org/10.1364/AO.49.004801.
[15] N. Schunk, K. Petermann, Stability analysis for laser diodes with short external cavities, IEEE Photon. Technol. Lett. 1 (1989) 49–51, https://doi.org/10.1109/68.4093.
[16] K. Petermann, External Optical Feedback Phenomena in Semiconductor Lasers, IEEE J. Sel. Top. Quantum Electron. 1 (1995) 480–489, https://doi.org/10.1109/2944.402500.
[17] R.W. Tkach, A. Chraplyvy, Regimes of feedback effects in 1.5-μm distributed feedback lasers, IEEE J. Lightwave Technol. 4 (1986) 1655–1661, https://doi.org/10.1109/JLT.1986.1074365.
[18] J. Kitching, Y. Shevy, J. Iannelli, A. Yariv, Reduction in Semiconductor Lasers using Optical Feedback with Dispersive loss, J. Lightwave Technol. 11 (1993) 1526–1532, https://doi.org/10.1109/50.244125.
[19] R. Lang, K. Kobayashi, External optical feedback effects on semiconductor injection laser properties, IEEE J. Quantum Electron. 16 (1980) 347–355, https://doi.org/10.1109/JQE.16.347.
[20] S. Donati, R.-H. Horng, The Diagram of Feedback Regimes Revisited, IEEE J. Sel. Top. Quantum Electron. 19 (2013) Art. no. 2234445. https://doi.org/10.1109/JSTQE.2012.2234445.
[21] J. Ohtsubo, Semiconductor Lasers: Stability, Instability and Chaos, 2nd ed., Springer, New York, USA, 2008.
[22] S. Donati, S.-K. Hwang, Chaos and High-Level Dynamics in coupled Lasers and their applications, Prog. Quantum Electron. 36 (2012) 293–341, https://doi.org/10.1016/j.pquantelec.2012.02.002.
[23] E. Randone, S. Donati, Self-mixing Interferometer: Analysis of the output Signals, Opt. Express 14 (2006) 9188–9196, https://doi.org/10.1364/OE.14.009188.
[24] Y. Yu, G. Giuliani, S. Donati, Measurement of the Linewidth Enhancement factor of Semiconductor Lasers based on the Optical Feedback Self-Mixing effect, IEEE Photon. Technol. Lett. 14 (2004) 900–902, https://doi.org/10.1109/LPT.2004.833778.
[25] Y. Yu, J. Xi, E. Li, J.F. Chicharo, Measuring the Linewidth Enhancement factor of Semiconductor Lasers with Weak Optical Feedback, Proc. SPIE 5628 (2005) 34–39, https://doi.org/10.1117/12.574324.
[26] H. Ludvigsen, M. Tossavainen, M. Kaivola, Laser linewidth measurements using self-homodyne detection with short delay, Opt. Commun. 155 (1998) 180–186, https://doi.org/10.1016/S0030-4018(98)00345-3.
[27] G. Giuliani, M. Norgia, Laser Diode Linewidth Measurement by Means of Self-Mixing Interferometry, IEEE Photon. Technol. Lett. 12 (2000) 1028–1030, https://doi.org/10.1109/68.898702.
[28] M. Norgia, D. Melchionni, S. Donati, Exploiting the FM-signal in a laser-diode SMI by means of a Mach-Zehnder filter, IEEE Photon. Technol. Lett. 29 (2017) 1552–1555, https://doi.org/10.1109/LPT.2017.2735899.
[29] P. Esmaili, M. Norgia, S. Donati, Noise Decrease in a Balanced Self-Mixing Interferometer: Theory and Experiments, IEEE Trans. Instrum. Meas. 72 (2023) 1–8, https://doi.org/10.1109/TIM.2023.3287259.
[30] Y. Zhao, Q. Wang, F. Meng, Y. Lin, S. Wang, B. Lin, S. Cao, Z. Fang, T. Li, E. Zang, 100-Hz Linewidth Diode Laser with External Optical Feedback, IEEE Phot. Techn. Lett. 24 (2012) 1795–1798.
[31] X.-G. Wang, B.-B. Zhao, F. Grillot, C. Wang, Spectral Linewidth Reduction of Quantum Cascade Lasers by Optical Feedback, J. Appl. Phys. 127 (2020), https://doi.org/10.1063/1.5124521.